Supporting Information

Probing the structural and magnetic properties of a new family of centrosymmetric dinuclear lanthanide complexes

Y. Jiang,[a] R. J. Holmberg, [a] F. Habib, [a] L. Ungur,[b,c] I. Korobkov,[a] L. F. Chibotaru,[b] and M. Murugesu*[a]

[a] *Department of Chemistry, University of Ottawa, 10 Marie Curie, Ottawa, ON, Canada K1N 6N5. E-mail: m.murugesu@uottawa.ca; Tel: +1 (613) 562 5800 ext. 2733*
[b] *Theory of Nanomaterials Group and INPAC Institute for Nanoscale Physics and Chemistry, Katholieke Universiteit Leuven, Celestijnenlaan, 200F, 3001 Leuven, Belgium.*
[c] *Temporary address: Theoretical Chemistry, Lund University, Getingevagen 60, 22241, Lund, Sweden.*

Table S1. Crystallographic data of the dinuclear complexes **1-4**.

	1	**2**	**3**	**4**
formula	$C_{36}H_{54}Gd_2N_6O_{11}$	$C_{36}H_{54}Dy_2N_6O_{11}$	$C_{36}H_{54}Ho_2N_6O_{11}$	$C_{18}H_{27}ErN_3O_{6.5}$
fw	1119.42	1129.92	1134.78	579.72
T/K	200(2)	200(2)	200(2)	200(2)
crystal system	Monoclinic	Monoclinic	Monoclinic	Triclinic
space group	$P2_1/n$	$P2_1/n$	$P2_1/c$	$P\bar{1}$
a/Å	11.3263(3)	11.3404(5)	11.2891(8)	8.5864(6)
b/Å	8.3727(2)	8.3937(3)	8.3607(6)	10.3618(8)
c/Å	20.7908(5)	20.8588(8)	20.7052(13)	11.2646(9)
α/deg	90	90	90	74.961(3)
β/deg	102.8720(11)	102.218(2)	102.908(4)	86.219(3)
γ/deg	90	90	90	78.632(3)
Vol/Å^3	2261.48(9)	2282.77(13)	2242.3(3)	1115.24(12)
Z	2	2	2	2
DC/ Mg m^{-3}	1.673	1.673	1.710	1.723
μ/mm^{-1}	2.976	3.314	3.572	3.799
Reflns collected	29945	35453	29375	8337
GOF	1.013	1.063	1.049	1.059
*R1, wR*2 (>2σ(I))[a]	0.0200, 0.0503	0.0492, 0.1028	0.0528, 0.1034	0.0381, 0.0959
*R1, wR*2 (all data)	0.0212, 0.0510	0.0765, 0.1112	0.0849, 0.1114	0.0421, 0.0987

[a] $R=R_1=||F_o| - |F_c||/\Sigma|F_o|$; $wR_2 = \{[\Sigma w(F_o^2-F_c^2)^2]/[w(F_o^2)^2]\}^{1/2}$; $w=1/[\sigma^2(F_o^2)+(ap)^2+bp]$, where $p=[\max(F_o^2,0)+2Fc^2]/3$.

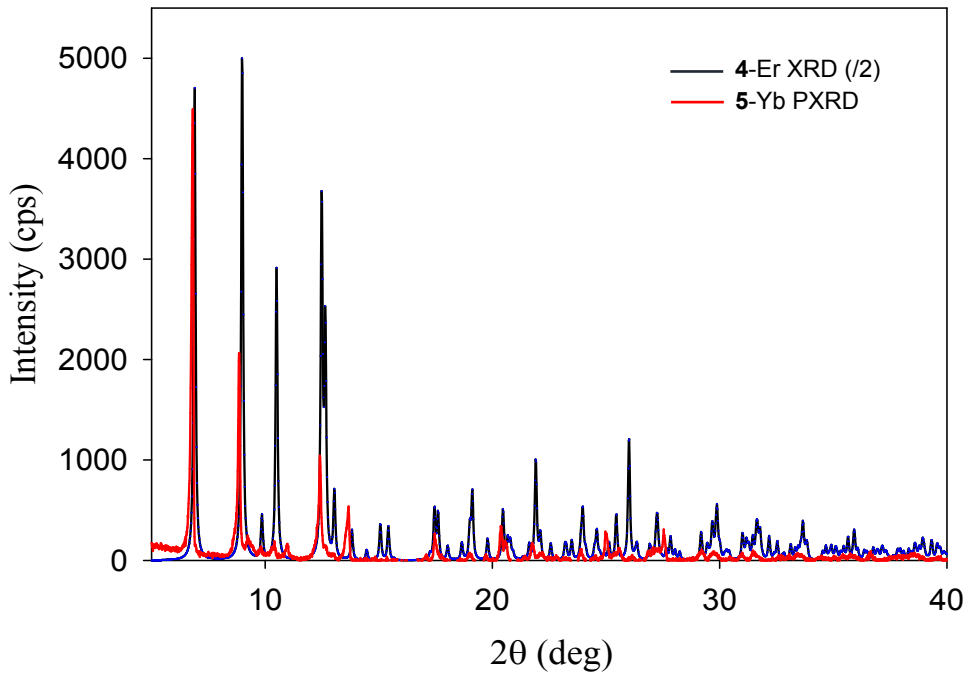

Figure S1. Powder X-ray diffraction comparison between the calculated pattern (dark blue) obtained from single crystal X-ray data of complex **4** and the experimental pattern (red) of complex **5** in the 5-40° 2*θ* region. The calculated pattern was divided by a factor of 2 for comparative purposes.

Table S2. Selected bond distances (Å) and angles (°) for complexes **1-4**.

	1	**2**	**3**	**4**
Ln1···Ln1a	4.0057(3)	3.9775(1)	3.9615(5)	3.9271(5)
Ln1-O3	2.3759(2)	2.3439(1)	2.330(4)	2.312(4)
Ln1-O3a	2.4292(1)	2.4085(1)	2.402(4)	2.377(4)
Ln1-O1	2.2951(2)	2.2713(1)	2.274(4)	2.248(4)
Ln1-O4	2.3196(2)	2.3008(1)	2.363(4)	2.282(4)
Ln1-O5	2.4001(2)	2.3848(1)	2.289(4)	2.360(5)
Ln1-O6	2.3607(1)	2.3446(1)	2.330(4)	2.320(4)
Ln1-N1	2.4940(2)	2.4464(1)	2.438(5)	2.426(4)
Ln1-N3	2.6292(2)	2.5969(1)	2.581(5)	2.565(5)
C9-O3	1.2657(1)	1.3083(0)	1.309(7)	1.311(6)
C9-N2	1.2943(1)	1.2901(0)	1.292(8)	1.300(7)
C8-N1	1.2712(1)	1.2859(0)	1.285(9)	1.288(8)
O3-O3a	2.640(2)	2.602(5)	2.589(6)	2.563(5)
Ln1-O3-Ln1a	112.941(3)	111.633(2)	111.7(2)	111.762(3)
O4- Ln1-O5	70.445(3)	71.066(1)	71.5(1)	71.621 (3)
Packing	8.379(1)	8.3937(5)	8.3607(7)	8.5864(7)

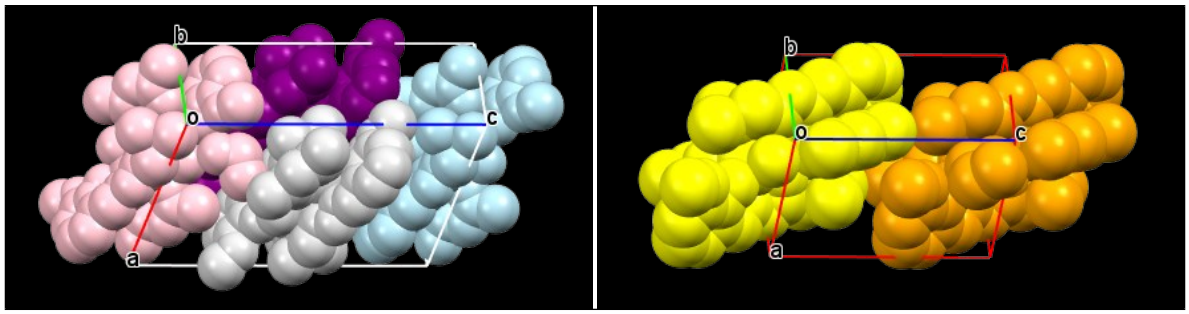

Figure S2. Spacefill packing diagrams of **1** (left) and **4** (right). Unit cell axes as shown.

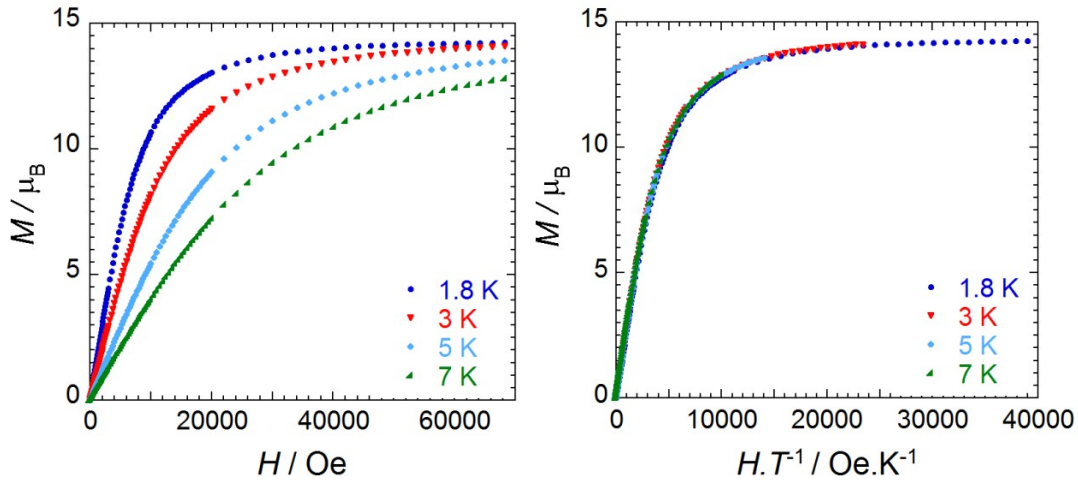

Figure S3. Field dependence of the magnetization *M* at 1.8, 3, 5, and 7 K for complex **1** plotted as *M vs. H* and *M vs. HT*$^{-1}$.

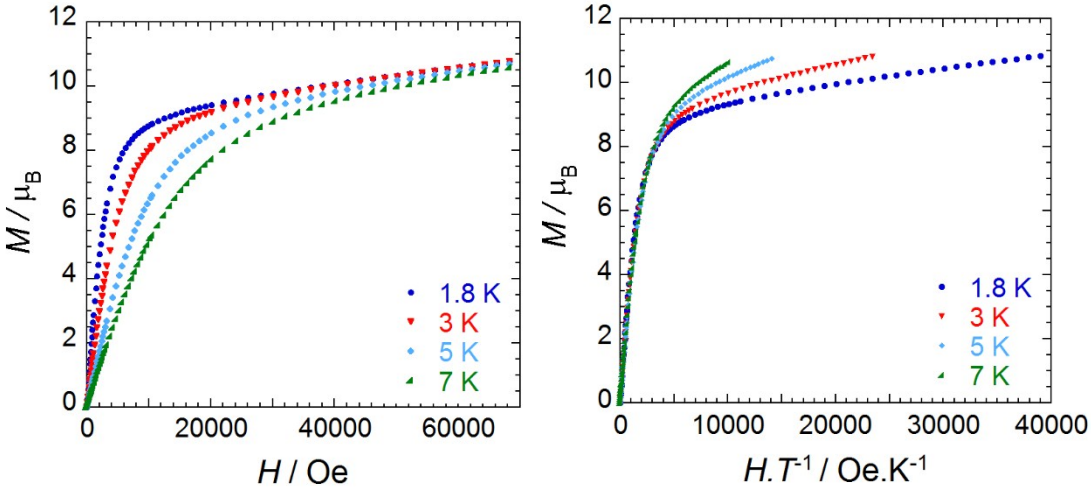

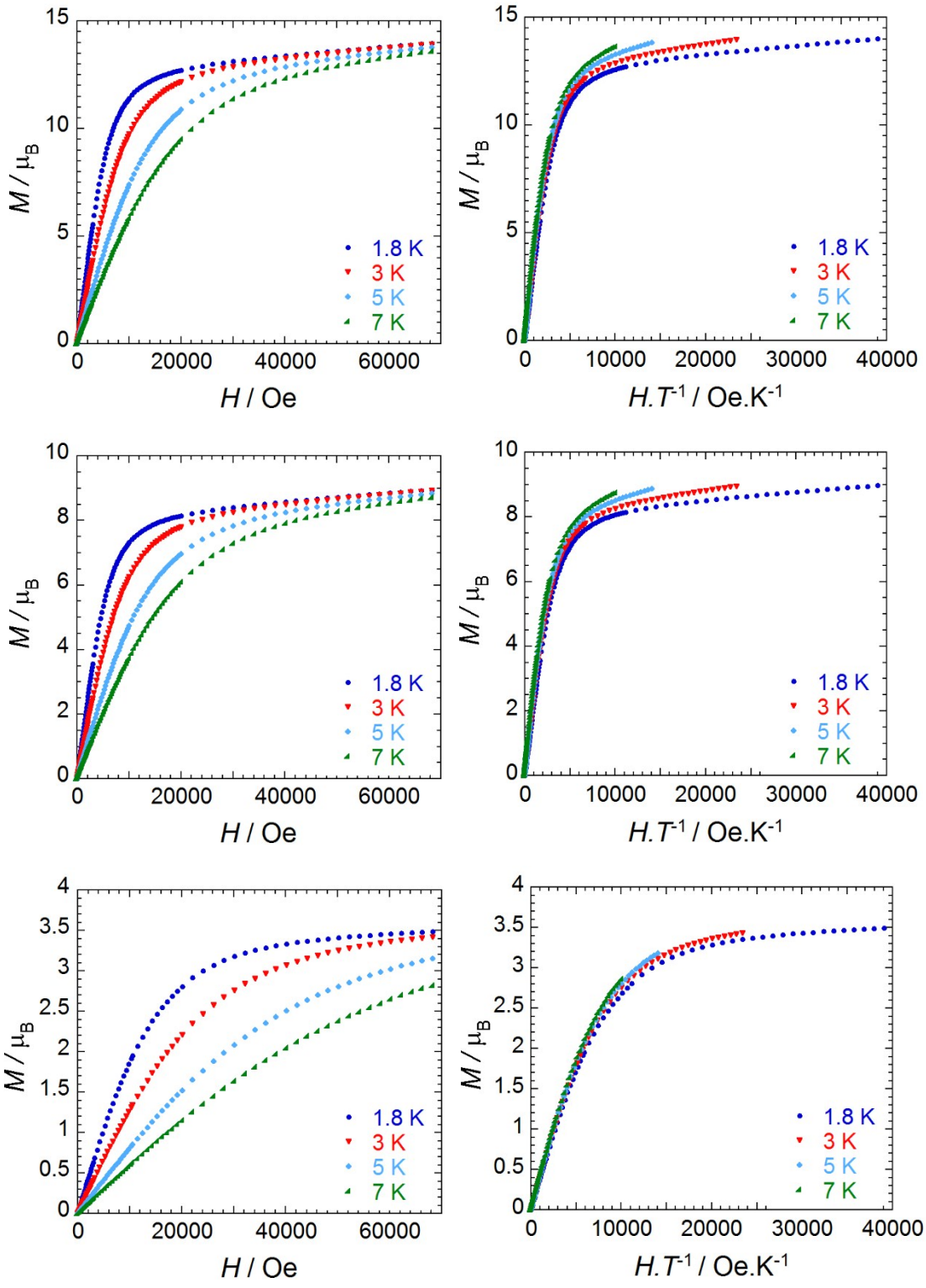

Figure S4. Field dependence of the magnetization *M* at 1.8, 3, 5, and 7 K for complexes **2-5** (top to bottom) plotted as *M vs. H* and *M vs.* HT^{-1}.

Table S3. Energies (cm^{-1}) of the low-lying Kramers doublets (KD) of the ***g*** tensor in the ground KD and the main values of the ***g*** tensor in the ground KD obtained within basis set 2* for complex **2**.

J multiplet	**Basis 1**	**Basis 2**
$^6H_{15/2}$	0	0
	79	76
	151	127
	204	197
	267	274
	351	362
	414	413
	499	513
Main Values of the ***g*** Tensor in the Ground KD		
$\boldsymbol{g}_X$	0.145	0.360
$\boldsymbol{g}_Y$	0.266	0.890
$\boldsymbol{g}_Z$	19.001	18.447

*Basis set 1: DZP quality (small-medium); Basis set 2: TZP quality (large).

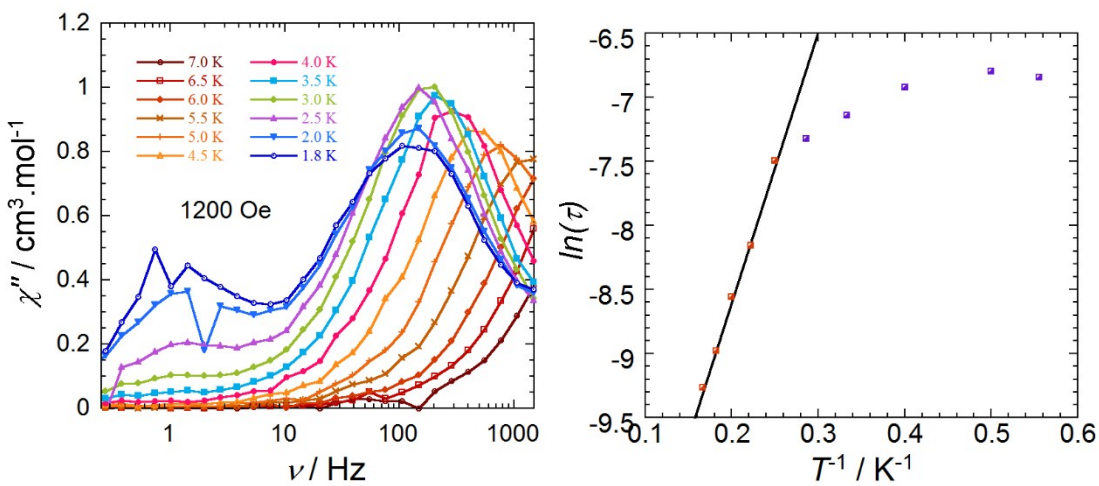

Figure S5. Left: Frequency (υ) dependence of the out-of-phase (χ'') magnetic susceptibility at the indicated temperatures for **4** under an applied static dc field of 1200 Oe. Bottom: Relaxation time of the magnetization *ln(τ) vs.* T^{-1} at applied dc field of 1200 Oe for complex **4**.The anisotropic barriers (obtained by fitting this data using the Arrhenius law, $\tau = \tau_0 \exp(U_{eff}/kT)$) were calculated to be U_{eff} = 21 K ($\tau_0 = 2.75*10^{-6}$ s).

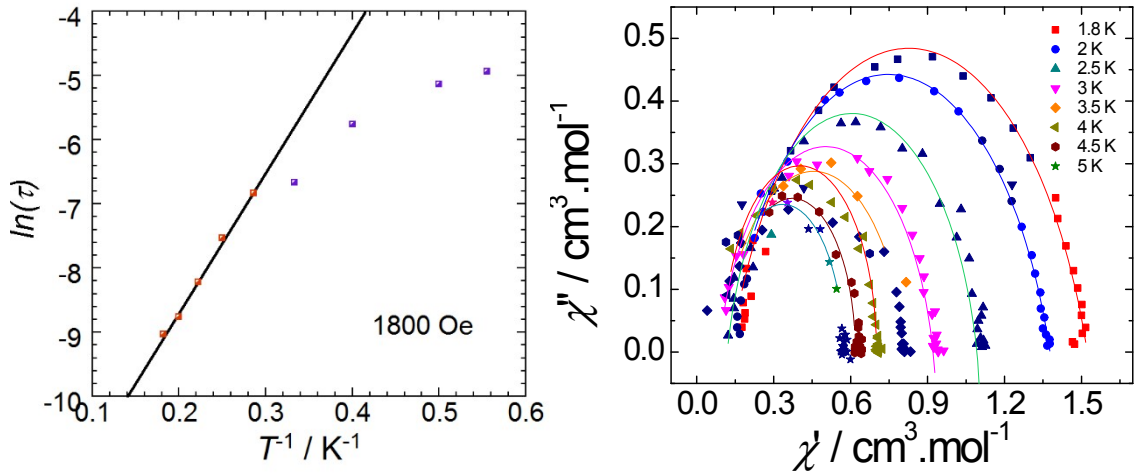

Figure S6. Left: Relaxation time of the magnetization *ln(τ) vs.* T^{-1} at an applied dc field of 1800 Oe for complex **5**.The anisotropic barriers (obtained by fitting this data using the Arrhenius law, $\tau = \tau_0 \exp(U_{eff}/kT)$) were calculated to be U_{eff} = 22 K ($\tau_0 = 2.13*10^{-6}$ s). Right: Cole-Cole plot using the ac susceptibility data.